SYMMETRIES,DYNAMICAL EVOLUTION OF PHASE TRANSITION AND NUGGET FORMATION

A. GOYAL
Department of Physics & Astrophysics,
University of Delhi, Delhi - 110 007, India.
agoyal@ducos.ernet.in

We study the influence of the presence of a magnetic field on chiral symmetry in the core of compact stars and in the early Universe. We find that the effect of a magnetic field is to enhance the chiral symmetry breaking in the sense that, in the presence of magnetic field, chiral symmetry gets restored at a higher temperature and density compared to the case where there is no magnetic field. However, the effect of a super strong magnetic field is to restore again chiral symmetry. We then investigate the dynamical evolution of the confinement-deconfinement phase transition in the expanding early Universe through bubble nucleation, taking into account reheating due to the heat released during the expansion of hadronic bubbles. We estimate the degree of supercooling and the time required to complete the phase transition. We then consider the formation of quark nuggets and their possible survival against boiling and evaporation to the present epoch.

1 Introduction

Spontaneous symmetry breaking is one of the most important concepts of all unified gauge theories. The idea that underlying symmetries of nature are larger than that of the vacuum plays a crucial role in the unification of forces. Of particular interest is the expectation that, at high temperatures, symmetries that are spontaneously broken today are restored and that during evolution, the Universe passed through a series of phase transitions from a higher symmetric phase to a lower symmetric phase associated with the spontaneous breakdown of gauge or perhaps global symmetry. In particular, at $t = 10^{-10}$s, when the temperature was $\sim 200GeV$, the Universe passed through the EWS breaking phase transition and later, at $t = 10^{-5}$s, $T = 200MeV$, there must have been a QCD phase transition from a QGP to confined hadronic matter and also to chiral symmetry breaking phase transition. Since the vacuum structure of SSB theories is very rich, topologically stable configurations of gauge and Higgs fields in the form of domain walls, cosmic strings and monopoles on the one hand and non-topological solitons like Q balls, quark nuggets, soliton stars on the other may exist and may have observable signatures. It is thus very instructive to investigate how the phase transition takes place in QFT in the environment of the early Universe and in

the core of neutron stars where temperature, density, external electromagnetic field and external gravity may all play important roles.

In GUTS, Higgs plays a most important role. They are fundamental scalars which give masses to fermions and gauge bosons through their VEVs. In theories like technicolor models, Higgs are composite of some fundamental fermion fields. QCD is an example of QFT which is invariant under chiral transformations at the Lagrangian level in the absence of quark mass matrix; the dynamics of QCD are expected to be such that chiral symmetry is dynamically broken with the vacuum state acquiring a non-zero quark-antiquark condensate $< \bar{q}q >$, and the Goldstone theorem then requires the existence of approximately massless pseudoscalar mesons. To study chiral phase transition in QCD, we need a non-perturbative treatment and a particularly attractive frame work to study is the Nambu-Jona-Lasino model. The linear Sigma model is another framework which has the advantage of being renormalizable in contrast to the NJL model which, in 4-D, is known to be non-renormalizable. An elegant and efficient way to study symmetry properties of vacuum at finite temperature and density in external environment is through the 'Effective Potential' approach discussed extensively in the literature. We compute here, in the one loop approximation, the effective potential in the presence of an external magnetic field and gravity at finite temperature and density in the framework of the linear sigma and NJL models, respectively. We then study the dynamic evolution of phase transition through bubble nucleation of the hadronic phase.

2 Chiral Symmetry in External Magnetic Field

It has also been suggested[1] that systems with spontaneously broken symmetries can make a transition from broken symmetric to restored symmetric phase in the presence of external fields. Large magnetic fields with strength up to 10^{18} gauss have been conceived to exist[2] at the time of supernova collapse inside neutron stars, in other astrophysical compact objects and in the early Universe. The effect of such a strong magnetic field on chiral phase transition is thus of great interest for baryon free quark matter in the early Universe and for high density baryon matter in the core of neutron stars. To study chiral phase transition in QCD we need a non-perturbative treatment. Lattice techniques and the Schwinger-Dyson equations provide specially powerful methods to study the chiral structure of QCD. A particularly attractive framework to study such systems is the linear sigma model originally proposed as a model for strong nuclear interactions. We will consider this as an effective

model for the low energy phase of QCD and will examine the chiral symmetry properties at finite density and in the presence of an external magnetic field. To fix ideas we consider a two flavor $SU(2) \times SU(2)$ chiral quark model given by the lagrangian.

$$\mathcal{L} = i\bar{\psi}\gamma^{\mu}\partial_{\mu}\psi - g\bar{\psi}(\sigma + i\gamma_5\vec{\tau}.\vec{\pi})\psi + \frac{1}{2}(\partial_{\mu}\sigma)^2 + \frac{1}{2}(\partial_{\mu}\vec{\pi})^2 - U(\sigma,\vec{\pi}) \qquad (1)$$

where ψ is the quark field, σ and $\vec{\pi}$ are the set of four scalar fields and g is the quark-meson coupling constant. The potential $\mathrm{U}(\sigma,\vec{\pi})$ is

$$U(\sigma,\vec{\pi}) = -\frac{1}{2}\mu^2(\sigma^2 + \vec{\pi}^2) + \frac{1}{4}\lambda(\sigma^2 + \vec{\pi}^2)^2\,. \qquad (2)$$

For $\mu^2 > 0$, chiral symmetry is spontaneously broken. The σ field can be used to represent the quark condensate, the order parameter for chiral phase transition and the pions are the Goldstone bosons. At the tree level, the sigma, pion and quark masses are given, respectively, by

$$m_{\sigma}^2 = 3\lambda\sigma_{cl}^2 - \mu^2; m_{\pi}^2 = \lambda\sigma_{cl}^2 - \mu^2; m_{\psi}^2 = g\sigma_{cl} \qquad (3)$$

where $\sigma_{cl}^2 = \frac{\mu^2}{\lambda} = f_{\pi}^2$. We compute here, in the one loop approximation, the effective potential in the presence of an external magnetic field which is defined through an effective action $\Gamma(\sigma,B)$ which is the generating functional of the one particle irreducible graphs. The effective potential is then

$$V_{eff}(\sigma,B) = V_0(\sigma) + V_1(\sigma,B) \qquad (4)$$

where $V_1(\sigma,B)$ is obtained from the propagator function, $G(\sigma,B)$, through the known relation $V_1(\sigma,B) = -\frac{1}{2i}Tr\log G(\sigma,B)$. Alternatively, one can compute the shift in the vacuum energy density due to zero-point oscillations of the fields considered as an ensemble of harmonic oscillators[3]. We thus require the energy eigenvalues(excitations) of particles in the magnetic which, in the absence of the anomalous magnetic moment for uniform static magnetic field in the z-direction for a particle of mass M, charge q and spin J, are

$$E(k_z,n,J_z) = \left(k_z^2 + M^2 + (2n + 1 - sign(q)\ j_z)\,|q|\,B\right)^2 \qquad (5)$$

where n represents the Landau levels.

The contribution of scalar particles of mass M to $V_1(M^2)$ after a Wick rotation is thus given by

$$V_1(M^2) = \frac{1}{2}\int \frac{d^4k_e}{(2\pi)^4} ln(k_e^2 + M^2 - i\epsilon)\,. \qquad (6)$$

In the presence of a magnetic field, all we need to do is to replace the phase space integral

$$\int \frac{d^4k_e}{(2\pi)^4} \rightarrow \frac{eB}{2\pi} \sum_{n=0}^{\infty} \frac{d^2k_e}{(2\pi)^2} \tag{7}$$

and the energy by expression (5) for charged particles. For a scalar field of charge $\pm e$, we thus have

$$\begin{aligned} V_1(M^2,B) &= \frac{eB}{4\pi} \sum_{n=0}^{\infty} \int \frac{d^2k_e}{(2\pi)^2}\ ln(k_e^2 + (2n+1)eB + M^2) \\ &= -\frac{eB}{4\pi}\ \frac{\partial}{\partial\alpha}\ \frac{\Gamma(\alpha - d/2)}{\Gamma(\alpha)(4\pi)^{d/2}} \sum_{n=0}^{\infty} \frac{1}{(M^2 + eB + 2neB)^{\alpha - d/2}} \Bigg|_{\alpha=0,d=2} \\ &= -\frac{eB}{4\pi}\ \lim_{\alpha\to 0}\ \frac{\partial}{\partial\alpha}\ \frac{\Gamma(\alpha - \frac{d}{2})}{\Gamma(\alpha)(4\pi)^{\alpha-\frac{d}{2}}} \frac{1}{(2eB)^{\alpha-\frac{d}{2}}}\ \zeta(\alpha - \frac{d}{2}, \frac{M^2+eB}{2eB}) \Bigg|_{\alpha=0,d=2} \end{aligned} \tag{8}$$

where $\zeta(z,q)$ is the generalized Riemann zeta function

$$\zeta(z,q) = \sum_{n=0}^{\infty} \frac{1}{(q+n)^z} = \frac{1}{\Gamma(z)} \int_0^{\infty} dt\ \frac{t^{z-1}e^{-qt}}{1-e^{-}t}\,. \tag{9}$$

The potential (8) has poles at α=0, 1 and 2 for d=2 which can be absorbed in the counter-terms. The finite part depends on the exact renormalization conditions that are imposed. In what follows we would use the $\overline{MS}$ renormalization scheme. From Eqs. (8) and (9) we can write

$$V_1(M^2,B) = -\frac{eB}{32\pi^2} \lim_{\alpha\to 0} \frac{\partial}{\partial\alpha} \frac{(2eB)^{1-\alpha}}{\Gamma(\alpha)} \int dt\ t^{\alpha-2}\ \frac{e^{-\frac{M^2}{2eB}t}}{\sinh\frac{t}{2}} \tag{10}$$

which converges for Re $\alpha > 2$. We analytically continue the result in the complex α-plane and use the dimensional regularization technique to extract its finite contribution. To proceed further we first consider the case $\frac{M^2}{2eB} < 1$, expand $e^{-\frac{M^2}{2eB}t}$ and formally integrate Eq. (10) to obtain

$$\begin{aligned} V_1(M^2,B) = -\frac{|q|\,B}{32\pi^2}\ \lim_{\alpha\to 0}\ \frac{\partial}{\partial\alpha}\ \sum_{n=0}^{\infty} (\frac{M^2}{2eB})^{\alpha+\nu-1} \frac{(-1)^\nu}{\nu!\ (M^2)^{\alpha-1}} \\ \frac{2}{\Gamma(\alpha)}(2^{\alpha+\nu-1} - 1)\ \Gamma(\alpha+\nu-1)\ \zeta(\alpha+\nu-1)\,. \end{aligned} \tag{11}$$

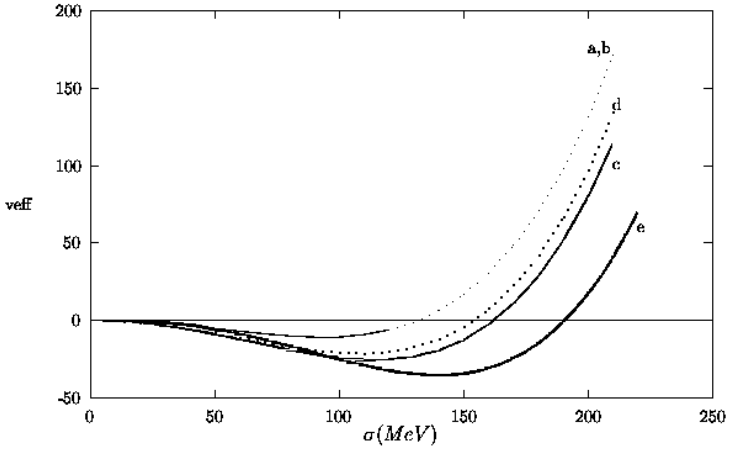

Figure 1. Effective potential in units of $(100MeV)^4$ as a function of $\sigma(MeV)$ for different values of the magnetic field. The curves a, b, c, d and e correspond to B=0, $10^{16}, 10^{18}, 10^{19}$ and 3×10^{19} Gauss, respectively.

Keeping leading terms in $\frac{M^2}{2eB}$, we obtain

$$V_1(M^2,B) = -\frac{1}{16\pi^2}\left[\frac{e^2B^2}{2\pi}\zeta(2)\log 2eB + \frac{eBM^2}{2}\log 2 - M^4\frac{\pi}{2}\log 2eB + ...\right]. \tag{12}$$

The leading term for the contribution of charged Goldstone bosons, relevant for symmetry considerations, is

$$V_1(M^2,B) \sim -\frac{eBM^2}{32\pi^2}\log 2\,. \tag{13}$$

For the case of $\frac{M^2}{2eB} > 1$ we write Eq. (10) as

$$V_1(M^2,B) = -\frac{1}{32\pi^2}\lim_{\alpha\to 0}\frac{\partial}{\partial\alpha}\frac{1}{\Gamma(\alpha)}\int_0^\infty dx\; x^{\alpha-3}e^{-M^2x}\frac{eBx}{\sinh eBx} \tag{14}$$

and keeping leading terms, we get

$$V_1(M^2,B) \simeq \frac{1}{64\pi^2}[M^4(\log M^2 - \frac{3}{2}) - \frac{2}{3}(eB)^2\log M^2]\,. \tag{15}$$

Likewise, for the charged fermion fields using Eq. (5) we obtain

$$V_1(M^2,B) = \frac{4\,|q|\,B}{32\pi^2}\lim_{\alpha\to 0}\frac{\partial}{\partial\alpha}\frac{(2\,|q|\,B)^{1-\alpha}}{\Gamma(\alpha)}\int_0^\infty dt\; t^{\alpha-2}e^{-\frac{M^2}{2|q|B}t}\coth\frac{t}{2}\,. \quad (16)$$

The factor 4 and the positive sign account for the spinor nature of the Fermi field. In the limits mentioned above, we have

$$V_1(M^2,B) = \frac{|q|\,BM^2}{8\pi^2}(1-\log M^2) \quad (17)$$

and

$$V_1(M^2,B) \simeq -\frac{1}{16\pi^2}[M^4\;(\log M^2-\frac{3}{2})+\frac{2}{3}\;(|q|\,B)^2\log M^2] \quad (18)$$

for $\frac{2|q|B}{M^2} > 1$ and < 1 respectively. To proceed further we first consider the case $\frac{M^2}{2eB} < 1$; keeping leading terms and adding the contributions of all the charged particles, the total $V_{eff}(\sigma,B)$ for the sigma model, at the one loop level, is thus given by[4]

$$\begin{aligned} V_{eff}(\sigma,B) = &-\frac{1}{2}\mu^2\sigma^2+\frac{\lambda}{4}\sigma^4+\frac{1}{64\pi^2}(3\lambda\sigma^2-\mu^2)^2\log(\frac{3\lambda\sigma^2-\mu^2}{m_\sigma^2}-\frac{3}{2}) \\ &+\frac{1}{64\pi^2}(\lambda\sigma^2-\mu^2)^2\log(\frac{\lambda\sigma^2-\mu^2}{m^2}-\frac{3}{2})-\frac{eB}{16\pi^2}(\lambda\sigma^2-\mu^2)\log 2 \\ &-\frac{N_c}{16\pi^2}\sum_{flav}[g^4\sigma^4(\log\frac{g^2\sigma^2}{m_f^2}-\frac{3}{2})+\frac{2}{3}(|q|\,B)^2\log\frac{g^2\sigma^2}{m_f^2}]\,. \end{aligned} \quad (19)$$

For $\frac{|q|B}{M^2} > 1$, the last term in Eq.(19) is replaced by $\frac{|q|BM^2}{8\pi^2}(1-logM^2)$ summed over quark flavors. In figure 1, we plot $V_{eff}(\sigma,B)$ as a function of σ for different values of the magnetic field and compare it with the case of zero magnetic field. As input parameters we choose the constituent quark mass m_f= 500 MeV, the sigma mass m_σ=1.2 GeV and f_π=93 MeV. We find that, in the presence of intense magnetic fields, chiral symmetry breaking is enhanced. For magnetic fields large compared to m_f^2, we observe that though the fermionic contribution is towards symmetry restoration, it is not enough to offset the contribution of charged Goldstone pions. In order to study chiral symmetry restoration, in the case of neutron stars, as a function of the chemical potential μ associated with finite baryon number density, we employ the imaginary time formalism by summing over Matsubara frequencies. This amounts to adding the fermionic free energy to the one loop effective potential and is given by

$$V_1^\beta(\sigma) = -\frac{\gamma}{\beta}\int\frac{d^3k}{(2\pi)^3}\;\ln\,(1+e^{-\beta(E-\mu)}) \quad (20)$$

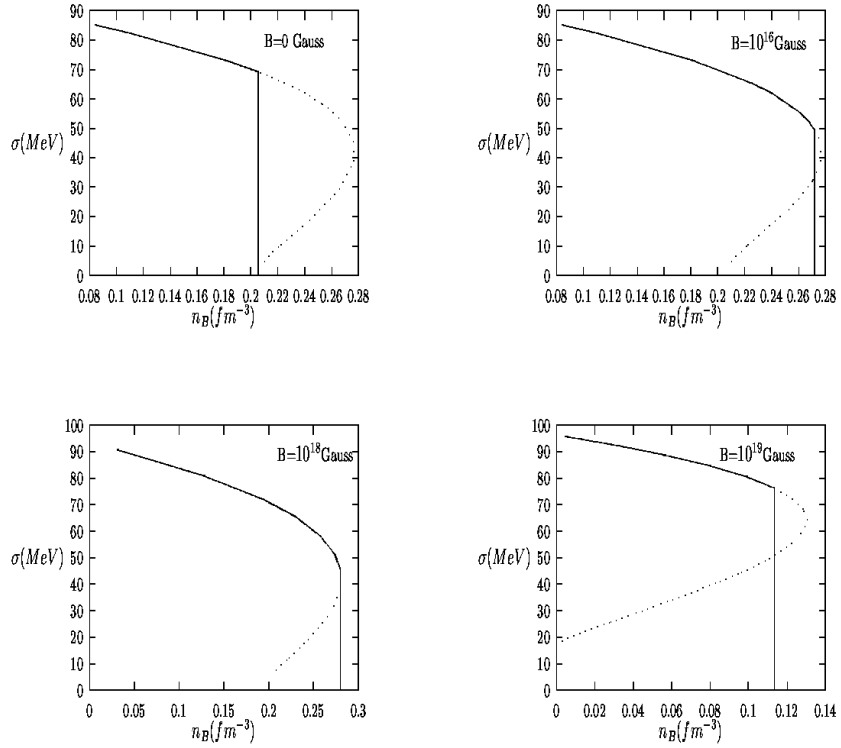

Figure 2. Chiral condensate $\sigma(MeV)$ as a function of baryon density in f_m^{-3} for $B = 0{,}10^{16}, 10^{18}$ and 10^{19} Gauss, respectively.

which, in the presence of a static uniform magnetic field, becomes

$$V_1^{\beta}(\sigma) = -\frac{\gamma}{\beta}\,\frac{eB}{2\pi}\sum_{n=0}^{\infty}\int_0^{\infty}\frac{dk_z}{2\pi}\;\ln\,(1+e^{-\beta(E-\mu)}) \tag{21}$$

where γ is the degeneracy factor and is equal to $2N_c$ for each quark flavor. We consider cold dense isospin symmetric quark matter for which the integrals can be performed analytically. The baryon number density corresponding to

the chemical potential μ is given by the usual thermodynamical relations.

$$N_B(\mu,0) = \frac{1}{3}\sum_{flav} \frac{\gamma}{6\pi^2}\ (\mu^2 - g^2\sigma^2)^{\frac{3}{2}} \tag{22}$$

and

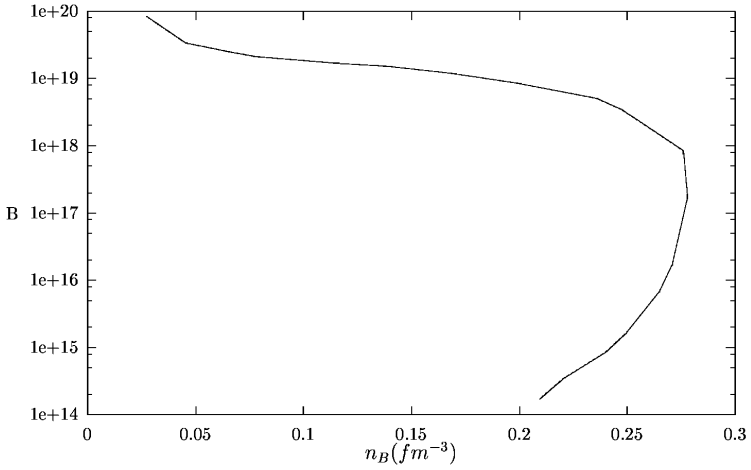

Figure 3. Phase diagram as a plot of the magnetic field (in Gauss) versus baryon density.

$$N_B(\mu,B) = \frac{1}{3}\sum_{n=0}^{n_{max}} \frac{\gamma\,|q|\,B}{4\pi^2}\ (2-\delta_{\mu,0})\ \sqrt{\mu^2 - g^2\sigma^2 - 2n\,|q|\,B} \tag{23}$$

for zero and finite magnetic field respectively. Here n_{max}= Int $\left|\frac{\mu^2-g^2\sigma^2}{2|q|B}\right|$. To study the chiral symmetry behavior at finite density in the presence of an uniform magnetic field, we minimize the effective potential with respect to the order parameter σ for fixed values of the chemical potential and magnetic field (which then fixes the baryon density). The results are shown in figure 2 where we have plotted the order parameter σ as a function of density at T=0 for different values of the magnetic field. The solution indicates a first order phase transition. The actual transition takes place at the point where the two minima of the effective potential, at σ=0 and σ=$\sigma(\mu$,B) non-zero, become degenerate. The lower values of σ (represented by dotted curves) are

unphysical in the sense that they do not correspond to the lowest state of energy. In figure 3 is plotted the phase diagram in the magnetic field-baryon density plane. We find that the magnetic field continues to enhance chiral symmetry breaking at low densities as expected but as the magnetic field is raised, chiral symmetry is restored at a much lower density compared to the free field finite density case.

3 Dynamical Evolution of Quark-hadron Phase Transition Through Bubble Nucleation

It is well known that a phase transition from a quark gluon plasma to confined hadronic matter must have occurred at some point in the evolution of the early Universe, typically at around $10 - 50\mu s$ after the Big Bang. This leads to an exciting possibility of the formation of quark nuggets through the cosmic separation of phases [5]. As the temperature of the Universe falls below the critical temperature T_c of the phase transition, the quark gluon plasma super cools and the transition proceeds through the bubble nucleation of the hadron phase. As the hadronic bubbles expand, they heat the surrounding plasma, shutting off further nucleation and the two phases coexist in thermal equilibrium. The hadron phase expands driving the deconfined quark phase into small regions of space and it may happen that the process stops after the quarks reach sufficiently high density to provide enough pressure to balance the surface tension and the pressure of the hadron phase. The quark matter trapped in these regions constitute the quark nuggets. The number of particles trapped in the quark nugget, its size and formation time are dependent sensitively on the degree of super cooling. The duration of the phase transition also depends on the expansion of the Universe and on other parameters like the bag pressure B and the surface tension σ.

The quark nuggets formed in the small super cooling scenario are in a hot environment around the critical temperature T_c and are susceptible to evaporation from the surface [6] and to boiling through subsequent hadronic bubble nucleation inside the nuggets [7]. However, in the large super cooling scenario we have the interesting possibility of these nuggets forming at a much lower temperature than T_c due to the long duration of the transition and consequent expansion of the Universe. Alcock and Farhi [6] have shown that the quark nuggets with baryon numbers $\leq 10^{52}$ and mass $\leq 10^{-5} M_{\odot}$ are unlikely to survive evaporation of hadrons from the surface. Boiling was shown to be even a more efficient mechanism of nugget destruction [7]. These results were somewhat modified by Madsen et.al.[8] by taking into account the

flavor equilibrium near the nugget surface for the case of evaporation and by considering the effect of interactions in the hadronic gas for the case of boiling. In the large super cooling scenario the time of formation of these nuggets can be quite late when the number of baryons in the horizon (of size $\sim 2t$) is large and temperature much lower. These nuggets can easily survive till the present epoch.

There have been recent observations by gravitational micro lensing[9] of dark objects in our galactic halo having masses of about $0.01 - 1$ solar mass. If these objects have to be identified with quark nuggets, they could only have been formed at a time later than the time ($\sim 50 - 100\mu s$) when the Universe cooled through T_c. When the early Universe as a quark-gluon thermodynamic system cools through the critical temperature T_c, energetically, the new phase remains unfavorable as there is free energy associated with the surface of separation between the phases. Small volumes of the new phase are thus unfavorable and all nucleated bubbles with radii less than the critical radius collapse and die out. But those with radii greater than the critical radius expand until they coalesce with each other. So super cooling occurs before the new phase actually appears and is then followed by reheating due to release of latent heat. The bubble nucleation rate[10] at temperature T is given by

$$I = I_o e^{-\frac{W_c}{T}} \tag{24}$$

where I_o is the prefactor having dimension of T^4. The prefactor used traditionally in early Universe studies[10] is given by

$$I_o = (\frac{W_c}{2\pi T})^{\frac{3}{2}} T^4 \,. \tag{25}$$

Csernai and Kapusta[11] have recently computed this prefactor in a coarse-grained effective field theory approximation to QCD and give

$$I_o = \frac{16}{3\pi}(\frac{\sigma}{3T})^{\frac{3}{2}} \frac{\sigma \eta_q R_c}{\xi_q^4 (\Delta w)^2} \tag{26}$$

where $\eta_q = 14.4T^3$ is the shear viscosity in the plasma phase, ξ_q is a correlation length of order 0.7 fm in the plasma phase and Δw is the difference in the enthalpy densities of the two phases. The critical bubble radius R_c and the critical free energy W_c are obtained by maximizing the thermodynamic work expended to create a bubble and are given by

$$R_c = \frac{2\sigma}{P_h(T) - P_q(T)} \tag{27}$$

and

$$W_c = 4\pi\sigma R_c^2(T)/3 = \frac{16\pi\sigma^3}{3\Delta P^2} \tag{28}$$

where

$$\Delta P = P_h(T) - P_q(T) \tag{29}$$

is the pressure difference in hadron and quark phase.

For simplicity we describe the quark matter by a plasma of massless u,d quarks and massless gluons without interaction. The long range non-perturbative effects are parameterized by the bag constant B. The pressure in the QGP phase is given by

$$P_q(T) = \frac{1}{3} g_q \frac{\pi^2}{30} T^4 - B \tag{30}$$

where $g_q \sim 51.25$ is the effective number of degrees of freedom. In the hadronic phase the pressure is

$$P_h(T) = \frac{1}{3} g_h \frac{\pi^2}{30} T^4 \tag{31}$$

where $g_h \sim 17.25$, taking the three pions as massless.

The fraction of the Universe $h(t)$ which has been converted to hadronic phase at the time t is given by the kinetic equation

$$h(t) = \int_{t_c}^{t} I(T(t'))[1 - h(t')]V(t', t)\left[\frac{R(t')}{R(t)}\right]^3 dt' \tag{32}$$

where $V(t', t)$ is the volume of a bubble at time t which was nucleated at an earlier time t' and $R(t)$ is the scale factor. This takes bubble growth into account and can be given simply as

$$V(t', t) = \frac{4\pi}{3}\left[R_c(T(t')) + \int_{t'}^{t} \frac{R(t)}{R(t'')} v(T(t''))dt''\right]^3 \tag{33}$$

where $v(T)$ is the speed of the growing bubble wall and can be taken to be

$$v(T) = v_o[1 - \frac{T}{T_c}]^{\frac{3}{2}} \tag{34}$$

where $v_o = 3c$. This has the correct behavior in that closer T is to T_c slower do the bubbles grow. When $T = \frac{2}{3}T_c$ we have $v(T) = \frac{1}{\sqrt{3}}$ the speed of sound of a massless gas. For $T < \frac{2}{3}T_c$ which occurs when there is large super cooling, we use the value $v(T) = \frac{1}{\sqrt{3}}$.

The other equation we need is the dynamical equation which couples time evolution of temperature to the hadron fraction $h(t)$. We use the two Einstein's equations as applied to the early Universe neglecting curvature

$$\frac{\dot{R}}{R} = \sqrt{\frac{8\pi G}{3}}\rho^{\frac{1}{2}} \; ; \; \frac{\dot{R}}{R} = -\frac{1}{3w}\frac{d\rho}{dt} \tag{35}$$

where $w = \rho + P$ is the enthalpy density of the Universe at time t. The energy density in the mixed phase is given by

$$\rho(T) = h(t)\rho_h(T) + [1 - h(t)]\rho_q(T)\,, \tag{36}$$

where ρ_h and ρ_q are the energy densities in the two phases at temperature T and similarly for the enthalpy. We numerically integrate the coupled dynamical equations (21),(23) and(24) to study the evolution of the phase transition starting above T_c at some temperature T corresponding to time t obtained by integrating the Einstein's Eqs. (25) and (26) in the quark phase. The number density of nucleated sites at time t, is given by

$$N(t) = \int_{t_c}^{t} I(t')[1 - h(t')]\left(\frac{R(t')}{R(t)}\right)^3 dt'\,. \tag{37}$$

Therefore, the typical separation between nucleation sites is $l_n = N(t)^{-1/3}$. This distance scale will eventually determine the number of quarks in a nugget.

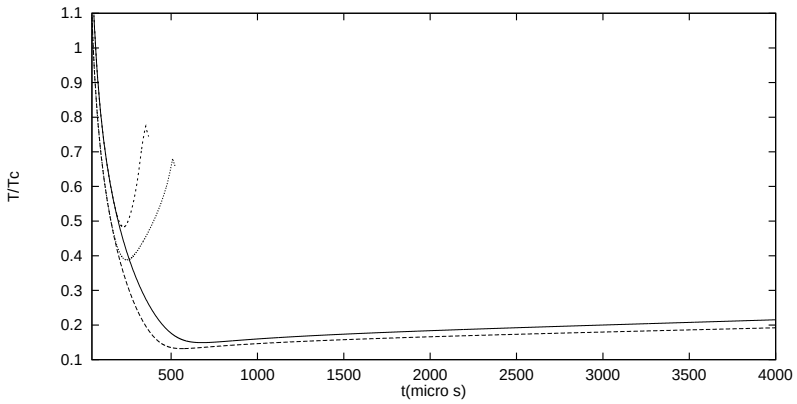

Figure 4. Temperature as a function of time. Solid and dashed curves are for $B^{1/4} = 100MeV$ and $\sigma = 39.5MeVfm^{-2}$ with the standard and the Kapusta pre-factors, respectively. Long dashed and dotted curves are for $B^{1/4} = 113MeV$ and $\sigma = 57.1MeVfm^{-2}$ with the standard and the Kapusta pre-factors, respectively.

$B^{1/4}$	σ	T_c	t_f	T_f	N_q	N_{qH}	l_n
MeV	$MeVfm^{-2}$	MeV	μs	MeV			m
235	50	169	12.1	169	2.6×10^{28}	7×10^{52}	8×10^{-3}
145	57.1	104.4	34.7	99.9	9.4×10^{35}	3.4×10^{53}	4.6
125	57.1	90	56.1	78.8	1.1×10^{39}	7.3×10^{53}	63
125	77	90	1511.8	17.9	6.3×10^{48}	1.6×10^{56}	4.9×10^{5}
100	39.5	71.9	2595	13.9	1.2×10^{50}	3.8×10^{56}	8.4×10^{5}
113	57.1	81.3	5138	12.3	9×10^{49}	2×10^{57}	1.7×10^{6}

Table 1. Some physical quantities for some representative values of B and σ.

To get an idea about the super cooling before nucleation begins, we can plot the nucleation time as a function of temperature, defined by

$$\tau^{-1}_{nucleation} = \frac{4\pi R_c^3}{3} I \,. \tag{38}$$

The quark number density is given by

$$n_q = \frac{2}{\pi^2}\zeta(3)(\frac{n_q}{n_\gamma})T^3 \tag{39}$$

where $\frac{n_q}{n_\gamma}$ is the quark to photon ratio estimated from the abundance of luminous matter in the Universe to be roughly equal to 3×10^{-10}. The quark nuggets have N_q quarks at time t given by the number of quarks in a volume $\frac{1}{N(t)}$, i.e. $N_q = \frac{n_q}{N(t)}$. The average temperature at which nuggets are formed when bubbles coalesce is obtained by finding the average time at which the expanding bubble surfaces meet. Assuming a cubic lattice, we have done this numerically to get the corresponding time t_f and temperature T_f for different values of B and σ.

Fig.4 shows the temperature as a function of time[12]. It is clear from this diagram that reheating takes place as nucleation starts with the release of latent heat. As σ increases, the super cooling is larger and reheating is slower. The transition takes much longer to complete with more chance of nugget formation. This allows the nuggets to be formed at a much lower temperature when bubble walls meet. For low supercooling there is rapid reheating, temperature reaches T_c and the phase transition is completed very swiftly with no chance of any nugget formation. Fig.5 shows the fraction $h(t)$ of the Universe in hadron phase as a function of time. For small values of σ the transition completes quickly as $h(t)$ goes to 1. But for larger σ it takes a

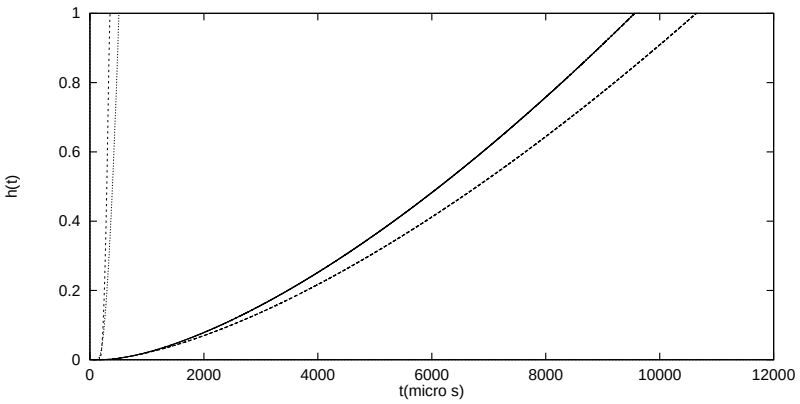

Figure 5. The hadron fraction as a function of time. Curves as in fig.4

larger time for $h(t)$ to become 1. The number of quarks in the horizon N_{qH} at time t is

$$N_{qH} \sim n_q(\frac{4}{3}\pi t^3) \sim (\frac{n_q}{n_\gamma})\frac{2\zeta(3)}{3\pi^2}T^3 4\pi t^3 \tag{40}$$

and we find that for all interesting cases $N_q \leq N_{qH}$ and this number is very sensitively dependent on the surface tension. Physically it is possible to have $N_{qH} \geq N_q \geq 10^{52}$ for some values of the parameters B and σ. In table 1 we list some physical quantities for some representative values of B and σ.

4 Conclusions

In conclusion we have examined the chiral symmetry behavior of the Linear Sigma model in the presence of a static, uniform magnetic field at the one loop level at zero density and at densities relevant in the core of neutron stars. We find that the contribution of scalar and fermion loops leads to an increase in chiral symmetry breaking. At high densities too, this effect persists and for magnetic fields of strength up to 10^{18} Gauss, there is enhancement in chiral symmetry breaking resulting in the restoration of symmetry at densities higher than if no magnetic field were present. However, in the case of an high magnetic field $B \geq 10^{19}$ Gauss, chiral symmetry is restored at lower densities. Thus, in the core of neutron stars, if the nuclear matter undergoes a transition

to deconfined quark matter, the presence of magnetic field would imply the existence of massive quark matter due to enhancement in chiral symmetry breaking. This would affect the equation of state and will have astrophysical implications.

Regarding the evolution of quark-hadron phase transition, detailed dynamics of the quark-hadron transition in the early Universe show that the evolution of the Universe does not necessarily follows the small super cooling scenario and certain choices of B and σ can have a bearing on the present state of the Universe. As nuggets with $N_q \geq 10^{52}$ are expected to survive the transition, they will contribute to the density of the Universe. We have explored in detail the possibility of nugget formation and also estimated their average separation, time of formation, quark content and survivability. Clearly, the analysis can be improved by taking interactions into account in both phases and also bubble interactions may be incorporated in the calculations, the qualitative results however are not expected to change. Thus if the nuggets studied above are indeed formed in a much cooler environment, they could contribute significantly to the missing mass in the Universe and be candidates for dark matter.

Acknowledgements

I would like to thank Deepak Chandra and Meenu Dahiya in whose collaboration most of this work has been done. I would also like to thank the organizers and participants of the workshop for providing the opportunity to present this work and for making the workshop stimulating and enjoyable.Partial support from the SERC scheme of Department of Technology (DST) Delhi is acknowledged.

References

1. See for example, A. D. Linde, Rep. Prog. Phys. **42**, 289 (1979); A. Salam and J. Strathdee, Nature **252**, 569 (1974).
2. I. M. Ternov and O. F. Dorofeev, Phys. Part.Nucl. **25**, 1 (1994); J. Daicic, N. E. Frankel and V. Kovalenko, Phys. Rev. Letts., **71**, 1779 (1993); C. Thompson and R. C. Duncan, Astrophys. Jour., **408**, 194 (1993); ibid **473**, 322 (1996); C. Kouveliotou et.al, Nature **393**, 235 (1998).
3. D. A. Kirshnitz and A. D. Linde, phys. Letts. B**42**, 471 (1972); S. Wienberg, Phys. Rev. **D9**, 3357 (1974); L. Dolan and R. Jakiew, Phys. Rev.

D9, 3320 (1974); C. Bernard, Phys. Rev. **D9** , 3312 (1974).
4. Ashok Goyal and Meenu Dahiya, Phys. Rev. **D62**, 025022 (2000).
5. E. Witten, Phys. Rev. **D30**, 272 (1984); A. Applegate and C.J. Hogan, Phys. Rev. **D31**, 3037 (1985); E. Farhi and R.L. Jaffe, Phys. Rev. **D30**, 2379 (1984).
6. C. Alcock and E. Farhi, Phys. Rev. **D32**, 1273 (1985).
7. C. Alcock and A. Olinto, Phys. Rev. **D39**, 1233 (1989); J.A. Frieman et.el., Phys. Rev. **D40**, 3241 (1989).
8. J. Madsen et.al., Phys. Rev. **D34**, 2947 (1986); J. Madsen and M.L. Olesen, Phys. Rev. **D43**, 1069 (1991).
9. C. Alcock et.al., Nature **365**, 621 (1993); E. Aubourg et.al., Nature **365**, 623 (1993).
10. C.J. Hogan, Phys. Lett. **B133**, 172 (1983); K. Kajantie and M. Kurki-Suonio, Phys. Rev. **D34**, 1719 (1996); G.M. Fuller,G.J. Mathews and C.R. Alcock, Phys. Rev. **D37**, 1380 (1988).
11. L.P. Csernai and J.I. Kapusta, Phys. Rev. Lett. **69**, 737 (1992); Phys. Rev. **D46**, 1379 (1992).
12. Deepak Chandra and Ashok Goyal, Phys. Rev. **D62**, 063505 (2000).